

Packing Modes of Distyrylbenzene Derivatives

Glenn P. Bartholomew,[†] Guillermo C. Bazan,^{*,†} Xianhui Bu,^{*,†} and
Rene J. Lachicotte[‡]

Department of Chemistry, University of California, Santa Barbara, California 93106, and
Department of Chemistry, University of Rochester, Rochester, New York 14627-0216

Received December 17, 1999. Revised Manuscript Received February 10, 2000

A range of 1,4-distyrylbenzene derivatives were synthesized and characterized by single-crystal X-ray diffraction to investigate the effects of substitution on the resulting crystal lattices. Molecules in this report include 1,4-bis(2,2-diphenylethenyl)benzene (**1**), 1,4-bis(1-cyano-2,2-diphenylethenyl)benzene (**2**), 1,4-bis(1-cyano-2-phenylethenyl)benzene (**3**), 1,4-bis(2,5-dimethoxystyryl)benzene (**4**), 1,4-bis(3,5-dimethoxystyryl)benzene (**5**), 2,5-difluoro-1-(pentafluorostyryl)-4-(4-*tert*-butylstyryl)benzene (**6**), and 1,4-bis(4-nitrostyryl)benzene·2DMF (**7**). The lattice of each is described and contrasted in light of distyrylbenzene derivatives previously reported. The results of thermal analysis by differential scanning calorimetry are included to further examine the effect of substitution on crystal properties.

Introduction

It is well appreciated that the distance and relative orientation between conjugated polymer chains and molecular chromophores play important roles in determining useful bulk qualities such as emission quantum yield and charge transport ability.¹ The level of order in many polymers, however, is low and prevents a detailed structure determination from diffraction experiments. In the area of electroluminescent polymers, specific side groups and functionalities have been introduced on the backbone to optimize electroluminescence quantum yields and facilitate processing by increasing solubility.² A wide range of polymer structures exist now for this purpose³ but the structural details of how these side groups influence interchain packing remain poorly understood. The absence of this information makes it difficult to deconvolute how the electronic structure of each polymer chain and the interchain coupling in the ensemble come together to determine the bulk properties.

The lattice properties of conjugated oligomers have been used to infer the interchain arrangement in polymers.⁴ In this approach, well-defined crystalline molecules are chosen which incorporate many of the structural features of the polymer under study. Examination of the lattice arrangement of the oligomers allows one to probe the arrangement of the conjugated segment as well as the influence of end groups. In addition, these studies can lead to the identification of molecules that are themselves useful as optoelectronic materials. Molecules studied in this way include sexithiophene,⁵

oligoquinones,⁶ distyrylbenzene,^{7,8} and larger poly(*p*-phenylenevinylene) (PPV) oligomers.⁹

In this contribution, we report on the lattice properties of a range of distyrylbenzene derivatives. These molecules may be considered representative of the poly(*p*-phenylenevinylene) (PPV) class of polymers which have found widespread use as components in organic light-emitting diodes. Distyrylbenzene derivatives have been studied as laser dyes,¹⁰ components of organic LEDs (oLEDs),¹¹ and as model compounds for the study of conductivity¹² and molecular properties^{13,14} in substituted PPV. The specific molecules under study in this report are 1,4-bis(2,2-diphenylethenyl)benzene (**1**), 1,4-bis(1-cyano-2,2-diphenylethenyl)benzene (**2**), 1,4-bis(1-cyano-2-phenylethenyl)benzene (**3**), 1,4-bis(2,5-dimethoxystyryl)benzene (**4**), 1,4-bis(3,5-dimethoxystyryl)benzene (**5**), 2,5-difluoro-1-(pentafluorostyryl)-4-(4'-*tert*-butylstyryl)benzene (**6**), and 1,4-bis(4-nitrostyryl)benzene·2DMF (**7**) (Chart 1). Compound **1** was chosen as a model of phenylated PPV which is under scrutiny for applications in conjugated polymer lasers.¹⁵ Compounds **2** and **3** contain the electron-withdrawing cyano group attached to the olefin and can also be seen as a model of

(5) Li, X.-C.; Siringhaus, H.; Garnier, F.; Holmes, A. B.; Feeder, S. C.; Clegg, W.; Teat, S. M.; Friend, R. H. *J. Am. Chem. Soc.* **1998**, *120*, 2206.

(6) Shetty, A. S.; Liu, E. B.; Lachicotte, R. J.; Jenekhe, S. A. *Chem. Mater.* **1999**, *11*, 2292.

(7) Wu, G.; Jacobs, S.; Lenstra, A. T. H.; Van Alsenoy, C.; Geise, H. J. *J. Comput. Chem.* **1996**, *17*, 1820.

(8) Irngartinger, H.; Lichtenthaler, J.; Herpich, R., *Struct. Chem.* **1994**, *5*, 283.

(9) Van Hutton, P. F.; Wildeman, J.; Meetsma, A. Hadziioannou J. *Am. Chem. Soc.* **1999**, *121*, 5910.

(10) Heller, A. *J. Chem. Phys.* **1964**, *40*, 2839.

(11) Tachelet, W.; Jacobs, S.; Ndayikengurukiye, H.; Geise, H. J. *Appl. Phys. Lett.* **1994**, *64*, 2364.

(12) Yang, Z.; Geise, H. J.; Mehbod, M.; Debrue, G.; Visser, J. W.; Sonneveld, E. J.; Van't dack, L.; Gijbels, R. *Synth. Met.* **1990**, *39*, 137.

(13) Renak, M. L.; Bartholomew, G. P.; Wang, S.; Ricatto, P. J.; Lachicotte, R. J.; Bazan, G. C. *J. Am. Chem. Soc.* **1999**, *121*, 7787.

(14) Strehmel, B.; Sarker, A. M.; Malpert, J. H.; Strehmel, V.; Seifert, H.; Neckers, D. C. *J. Am. Chem. Soc.* **1999**, *121*, 1226.

[†] University of California, Santa Barbara.

[‡] University of Rochester.

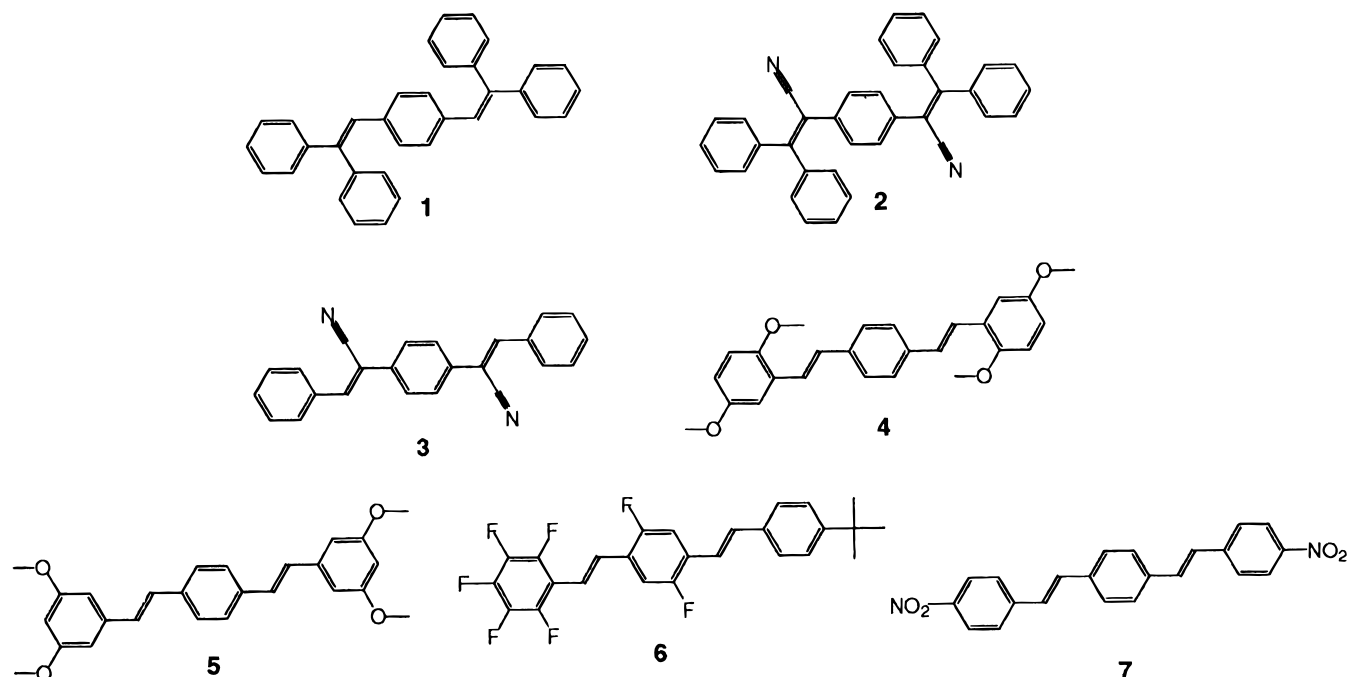
(1) Conwell, E. *Trends Polym. Sci.* **1997**, *5*, 218.

(2) Denton, D. J.; Tessler, N.; Harrison, N.; Friend, R. H. *Phys. Rev. Lett.* **1997**, *78*, 733.

(3) Kraft, A.; Grimsdale, A. C.; Holmes, A. B. *Angew. Chem., Int. Ed. Engl.* **1998**, *37*, 402.

(4) Enkelmann, V. In *Electronic Materials: The Oligomer Approach*; Mullen, K., Wegner, G., Eds.; Wiley-VCH: Weinheim, 1998.

Chart 1. Molecules under Study in This Report



cyano-substituted PPV (CN-PPV).^{16,17} Compounds **4** and **5** probe the differences in solid-state structure with a change in the end ring methoxy substitution (2,5 to 3,5). Compound **6** was chosen to examine the importance of phenyl-perfluorophenyl interactions in the resulting lattice arrangement and serves as a model of possible interactions in copolymers featuring aryl fluorine substitution.^{18,19} Compound **7** will be useful to illustrate the consequences of a strong electron-withdrawing group.

The single-crystal X-ray structure of each is discussed with a focus on the perturbation on the lattice arrangement by functionalization. Related structures found in the Cambridge Structural Database are included where pertinent to demonstrate the diversity of packing motifs found for the relatively simple distyrylbenzene framework. Results of thermal analysis are also presented in the context of energy requirements for different packing motifs.

Results and Discussion

In this section, we detail the structural features of compounds **1–7**. All molecules showed normal intramolecular metrical parameters. The focus of the discussion will be on lattice properties.

1,4-Bis(2,2-diphenylethenyl)benzene (1). The single-crystal X-ray diffraction study of molecule **1** indicates that there are two molecules per unit cell which are not related by crystallographic symmetry (i.e., the inversion center) (Figure 1). Instead, the crystal-

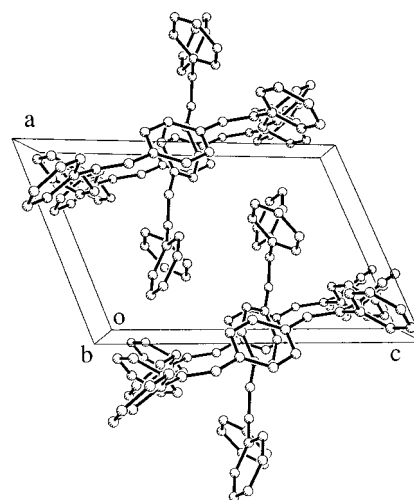


Figure 1. Packing diagram of 1,4-bis(2,2-diphenylethenyl)benzene(**1**) viewed down the *b* axis.

lographic symmetry element coincides with the molecular symmetry element of each molecule so that for each molecule, only half of it is crystallographically unique. Thus, there exist two groups of molecules that are independent of each other and are not related by symmetry elements. One group of these molecules is located at the center of the unit cell *c* axis while the other group of molecules is located at the unit cell face (the *bc* plane) center.

The terminal phenyl rings are not coplanar with the central ring. For one of the independent molecules, the ring trans to the central ring makes an angle of $\sim 63.3^\circ$ to the central ring plane while the ring cis to the central ring makes an angle of $\sim 60.5^\circ$. Such a conformation does not allow for the central phenyl rings in adjacent molecules to achieve cofacial stacking.

Adjacent intermolecular rings are arranged such that the face of one ring typically sees the edge of its neighbor. Angles between terminal phenyls of neighbor-

(15) Hennecke, M.; Damerau, R.; Muellen, K. *Macromolecules* **1993**, *26*, 3411.

(16) Greenham, N. C.; Moratti, S. C.; Bradley, D. D. C.; Friend, R. H.; Holmes, A. B. *Nature* **1993**, *365*, 628.

(17) Staring, E. G. J.; Demandt, R. C. J. E.; Braun, D.; Rikken, G. L. J.; Kessner, Y. A. R. R.; van Knippenberg, M. M. F.; Bouwmans, M. *Synth. Met.* **1995**, *71*, 2679.

(18) Gurge, R. M.; Sarker, A. M.; Lahti, P. M.; Hu, B.; Karasz, F. E. *Macromolecules* **1997**, *30*, 8286.

(19) Benjamin, I.; Faraggi, E. Z.; Avny, Y.; Davidov, D.; Neumann, R. *Chem. Mater.* **1996**, *8*, 352.

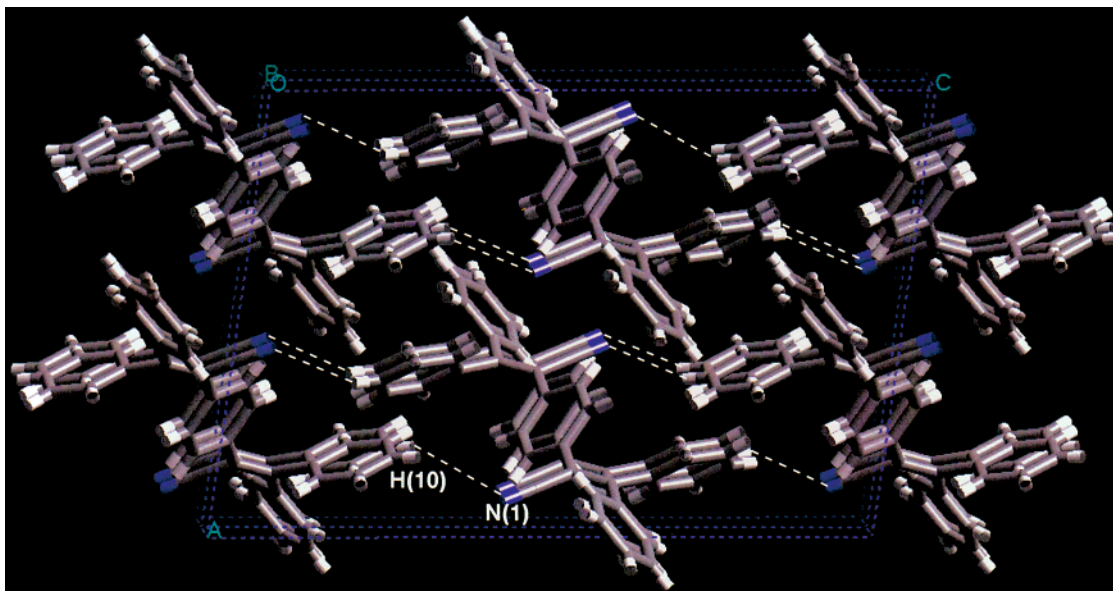


Figure 2. Packing diagram of 1,4-bis(1-cyano-2,2-diphenylethynyl)benzene (**2**) viewed down the *b* axis. Annotated close contacts are of a distance of 2.75(4) Å.

ing molecules are arranged nearly perpendicular ($\sim 80.5^\circ$, $\sim 78.5^\circ$). Viewed along the *b* axis (Figure 1), these terminal rings form a chain of T-like interactions that one might expect from the structure of benzene.²⁰ In contrast, when rotation of the terminal phenyls is restricted as in 1,4-bis(9-vinylfluorenyl)benzene²¹ (**PMYDFL**), molecules begin to form layers of cofacially stacked terminal fluorenes. The end units in **PMYDFL**, however, are nearly perpendicular with the fluorenes of neighboring stacks. With a more planar end group, the packing in **PMYDFL** begins to feature cofacial stacking balanced by the edge-to-face interactions seen in **1**.

1,4-Bis(1-cyano-2,2-diphenylethynyl)benzene (2). The molecular packing is considerably more symmetrical ($C2/c$ (no. 15)) for the cyano-substituted structure relative to **1** ($P\bar{1}$ (no. 2)). In this structure, only half of a molecule is crystallographically unique because each molecule is located at the crystallographic (4c) site (Figure 2). The volume occupied by each molecule is 649 Å³ compared to 603 Å³ for structure **1** and is the highest among the seven new structures reported here.

With the inclusion of cyano substitution on the olefin an improved registry between molecules is observed within the lattice. Examination of Figure 2 shows a weak contact between the cyano nitrogen and a hydrogen on a terminal ring (N(1)···H(10), ~ 2.75 Å). This interaction extends throughout the lattice and brings each molecule into contact with four others. Again, adjacent phenyl rings between molecules are close to perpendicular relative to one another. The angular relationship between end rings in **2** approaches the limit of the T-like junction seen in benzene.²⁰

1,4-Bis(1-cyano-2-phenylethynyl)benzene (3). Among all seven 1,4-distyrylbenzene (DSB) derivatives reported here, **3** is the only one with orthorhombic crystal symmetry ($Pbca$). The long molecular axes are

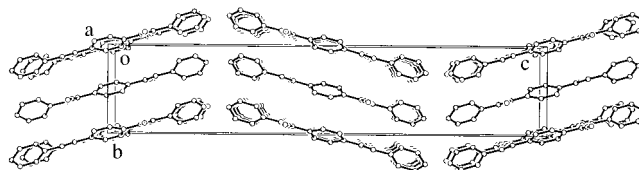


Figure 3. Packing diagram of 1,4-bis(1-cyano-2-phenylethynyl)benzene (**3**) viewed down the *a* axis.

not aligned in the same direction because of the point group symmetry operation (Figure 3). Like other structures reported here, each molecule is located at the crystallographic inversion center and only half of the molecule is crystallographically unique. Molecules are located either at the unit cell origins or at the unit cell face centers (all of the six faces). The molecule is highly nonplanar with cyano groups located neither in the plane of the central nor terminal rings. The angle between the terminal phenyl ring and the central phenyl ring is $\sim 56.8^\circ$.

Without the *cis*-substituted phenyl ring, the molecules in this structure are able to approach each other more closely. The weak N···H···C contact seen in **2** becomes much shorter in **3** (N(1)···H(7)–C, ~ 2.49 Å, see Figure 4) and falls well within the sum of van der Waal radii (~ 2.74 Å). This network of contacts leads to each molecule interacting with two others in the lattice and may be responsible for the increase in density (1.280 g/cm³) relative to **2** (1.241 g/cm³). Besides the N···H···C interaction, neighboring phenyl rings from different molecules arrange themselves to optimize T-type contacts.

1,4-Bis(2,5-dimethoxystyryl)benzene (4). As in **2** and **3**, the asymmetric unit of **4** corresponds to half a molecule. Molecules can be divided into two groups, one with the molecular center located at the middle of the crystallographic *b* axis and another with the molecular center sitting at the unit cell face (the *ac* plane) center (Figure 5). Two types of columns are formed when molecules stack along the *a* axis. Molecules in these two types of columns are at different heights along the *a* axis, one at $x = 0$ and the other at $x = 0.5$. The distance

(20) For a discussion on aryl stacking motifs, see: Williams, J. H. *Acc. Chem. Res.* **1993**, *26*, 593.

(21) Zobel, D.; Ruban, G.; Wendling, W. *Acta Crystallogr., Sect. B* **1979**, *35*, 1170.

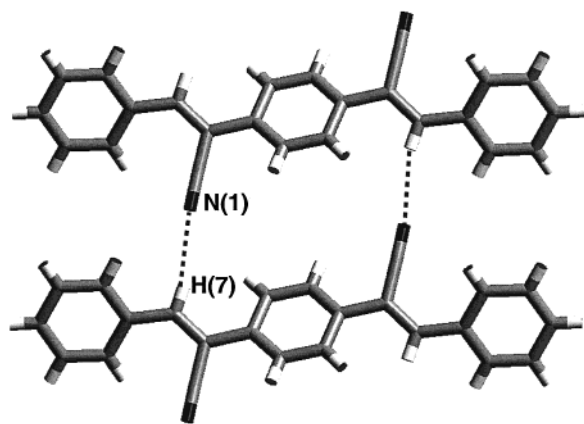


Figure 4. A layer of the structure of 1,4-bis(1-cyano-2,2-diphenylethenyl)benzene (**3**) roughly in the *bc* plane. Annotated close contacts are 2.49(4) Å.

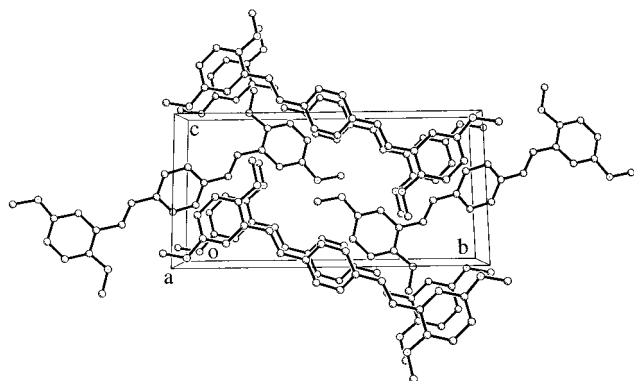


Figure 5. Packing diagram of 1,4-bis(2,5-dimethoxystyryl)benzene (**4**) viewed down the *a* axis.

between molecules along a given column is equal to the unit cell *a* axial length. The long axes of molecules in both groups are not parallel so that the terminal group of one molecule points toward the middle area between two molecules of adjacent columns.

Perhaps the most prominent feature in **4** is the network of close contacts that form a brick-like arrangement throughout the lattice. As shown in Figure 6 the distance of ~ 2.56 Å between O(2) and H(12) is consistent with the sum of the van der Waal radii (~ 2.60 Å). Each molecule makes contacts of this type with four other molecules. The "ortho" methoxy (O(1)) does not interact strongly with neighboring molecules but points the lone pairs on O toward the olefin on the same molecule (O(1) \cdots H(9)–C, 2.46 Å). The intermolecular O \cdots H interaction in **4** is not present in the lattice of 1,4-distyryl 2,5-dimethoxybenzene (**HESMUN**) or any of the chlorinated derivatives of 1,4-distyryl-2,5-dimethoxybenzene.^{7,8}

The lack of this contact in 1,4-bis(3,4,5-trimethoxystyryl)benzene²² (**JACBIY**) is noteworthy. Although **JACBIY** still features methoxy substitution at the 5 position of the terminal ring, the additional methoxy substitution leads to an environment at the end of the molecule that must minimize repulsive interactions between methoxy oxygens. The result is packing that is truly herringbone in nature with respect to the distyrylbenzene framework. For **4**, the absence of the

methoxy group at the 4 position as in **JACBIY** results in a lattice that is intermediate between herringbone and cofacially stacked.

1,4-Bis(3,5-dimethoxystyryl)benzene (5). The crystal structure of **5** is different from all of the above structures (**1–4**) in one important aspect: all molecules are oriented in the same direction (Figure 7). As in **2–4**, only half of the molecule is crystallographically unique and different molecules are related to one another by unit cell translational symmetry. An interesting observation is that all unit cell axes are relatively short (< 10 Å) because the long molecular axis is oriented approximately along the unit cell body diagonal direction.

Again, a network of O \cdots H–C contacts appears in **5** but with some important differences from **4** (Figure 8). Each molecule in **5** forms O \cdots H–C contacts with two other molecules instead of four as in compound **4**. Also, the "meta" methoxy of **5** cannot interact intramolecularly with the olefinic C–H as is the "ortho" methoxy in **4**. Instead, both methoxy methyls on the terminal ring of **5** face into the methoxy groups of the ring related by inversion (C(12) \cdots C(13), 3.40 Å). This arrangement between the methoxy methyls leads to more efficient packing indicated by an increase in density for **5** (1.303 g/cm³) relative to **4** (1.273 g/cm³). With the O \cdots H–C contact network, these "loose" stacks along the *b* axis are the units of the brick-like packing. Note that in **4**, the molecules themselves are the largest unit in the brick-like arrangement.

2,5-Difluoro-1-(pentafluorostyryl)-4-(4-*t*-butylstyryl)benzene (6). Among the seven derivatives reported here, **6** is the only molecule that lacks the symmetry of an inversion center and therefore it is not located on any symmetry site. Unlike **1–5**, the terminal phenyl rings are coplanar with the central phenyl rings. This stereochemistry contributes to the formation of columns along the *a* or *b* axes (Figure 9). Columns along the *a* axis consist of molecules in the same orientation and the distance between them is equal to the *a* axial length of ~ 6.12 Å (Figure 9a). Alternatively, molecules can be viewed as forming columns along the *b* axis (Figure 9b). Along the *b* direction, two adjacent molecules are related by a center of inversion and thus have opposite orientations. The bulky terminal alkyl groups in adjacent molecules are therefore not directly on top of each other.

The cofacial stacks formed along the *b* axis are joined at the ends by meshing of the butyl groups and laterally by a network of C–H \cdots F–C contacts. The lateral close contacts present are F(8) \cdots H(9) (~ 2.69 Å) and F(3) \cdots H(14) (~ 2.66 Å) (Figure 10).²³ This layered lattice is common among fluorinated distyrylbenzene derivatives.¹³ The major difference between the structure of **6** and previously characterized lattices of fluorinated DSB compounds is the parallel relationship between the molecular long axes in adjacent stacks. It has been shown that symmetric fluorination on the DSB framework leads to F \cdots F and H \cdots H along the end of the stacks.¹³ To minimize these contacts, the molecular long axes of the stacks, as well as an angle between the plane of molecules in adjacent stacks, are offset. The asymmetric substitution of **6** allows for an alternating ar-

(22) Verbruggen, M.; Zhou, Y.; Lenstra, A. T. H.; Geise, H. J. *Acta Crystallogr., Sect. C* **1988**, *44*, 2120.

(23) The estimated error in the intermolecular contact measurements is ± 0.04 Å.

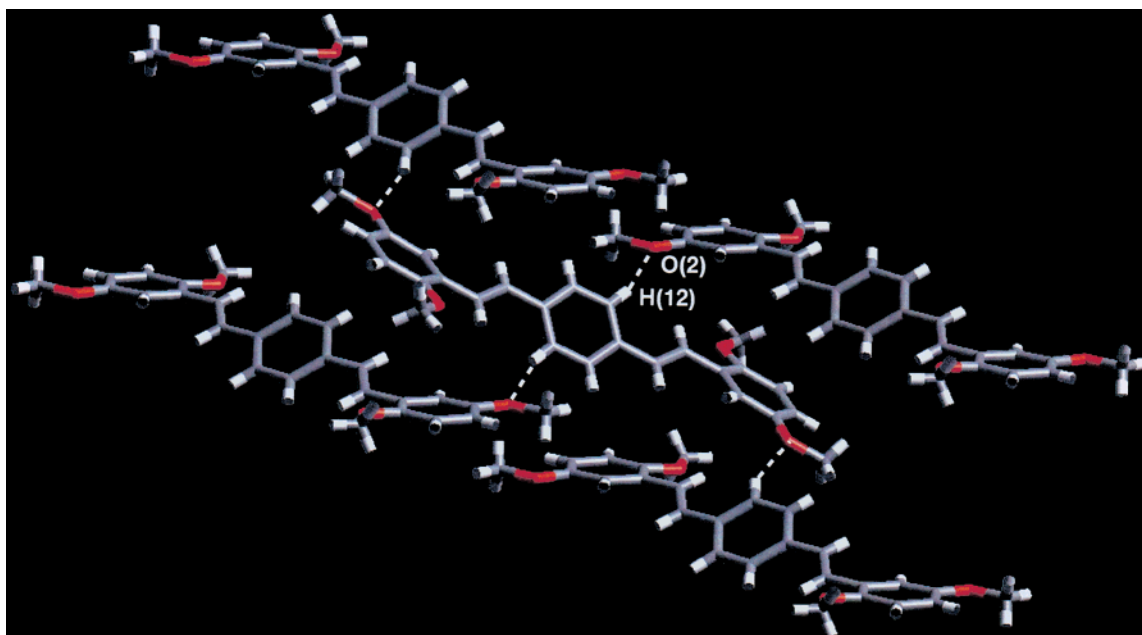


Figure 6. A layer of the structure of 1,4-bis(2,5-dimethoxystyryl)benzene (**4**) roughly in the *bc* plane. Annotated close contacts are of a distance of 2.56(4) Å.

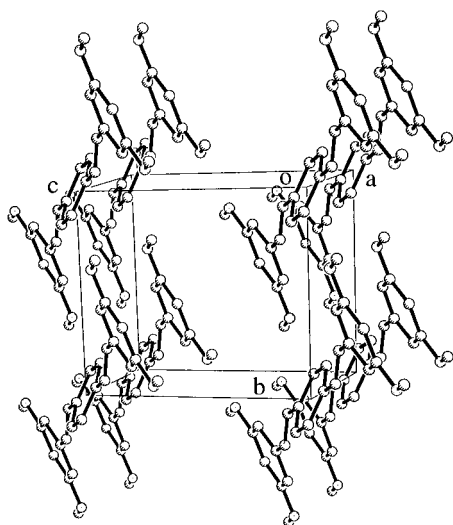


Figure 7. Packing diagram of 1,4-bis(3,5-dimethoxystyryl)benzene (**5**) viewed down the *a* axis.

rangement leading to a productive registry between the end environments of the molecules.

1,4-Bis(4-nitrostyryl)benzene·2 *N,N*-Dimethylformamide (7·(DMF)₂). The low solubility of this compound has prevented obtaining crystals suitable for diffraction studies from typical organic solvents such as ethanol or acetone. Single crystals were obtained by boiling **7** in *N,N*-dimethylformamide (DMF) and allowing the solution to cool slowly. In the lattice there are two DMF molecules for each of **7**. Similar to **6**, but very different from **1–5**, the terminal phenyl rings are coplanar with the central phenyl rings (Figure 11). Like other centrosymmetric molecules, **7** is located at the inversion center in the middle of the unit cell *a* axis.

Molecules of **7** form stacks along the crystallographic *a* axis. Within each stack, the repeat distance between two adjacent molecules is equal to the *a* axial length (~5.90 Å). DMF is held in channels that run along the *a* axis. Figure 12 shows a packing diagram with the

solvent molecules removed to illustrate better these channels. Close contacts are evident between DMF and **7** (Figure 13). The oxygen of DMF forms a bifurcated contact with **7** between a terminal phenyl H and an H on the olefin (O(3)···H(8), 2.35 Å; O(3)···H(13), 2.64 Å). Additionally, the distance between the nitro oxygen and a methyl H on DMF appears to be significant (O(2)···H(14A)—C, ~2.70 Å). It should be noted that inclusion of different small polar solvent molecules has also been demonstrated for the azo dye 3-hydroxy-6-(4'-nitro)-phenylazopyridine.²⁴

Edge–edge ring interactions between phenyl groups with the same substitution has been avoided in all of the structures shown thus far. The lattice of **7** is no exception but with one important difference. The interaction is avoided by cofacial overlap of the two NO₂ substituted phenyls rather than an angled deflection of the ring. When viewed down the *b* axis the terminal rings overlap in such a way that the NO₂ group is close to the olefin of its neighbor, completely avoiding other NO₂ moieties. However, these layers are again formed by molecules with a large offset from one another, leading to loose stacking. The **7**·DMF₂ lattice has the highest density of any of the structures reported here (1.329 g/cm³). The two small solvent molecules per unit cell make efficient use of residual space in the lattice.

Differential Scanning Calorimetry Analysis

Table 3 contains a summary of differential scanning calorimetry (DSC) analysis for compounds **1–7**. Comparison of the data of **1** and **2** shows a large difference in their *T*_ms which is consistent with the addition of four N···H—C interactions per molecule of **2**. The *T*_m for **3** is lower than **2** but is still relatively high. Compound **3** contains a similar network of N···H—C interactions but is smaller in size with respect to **3**. Intermolecular contacts in **4** consist of interactions with the methoxy O which provides a less polar environment for hydrogen bonding than **3**, resulting in a lower melting point. The

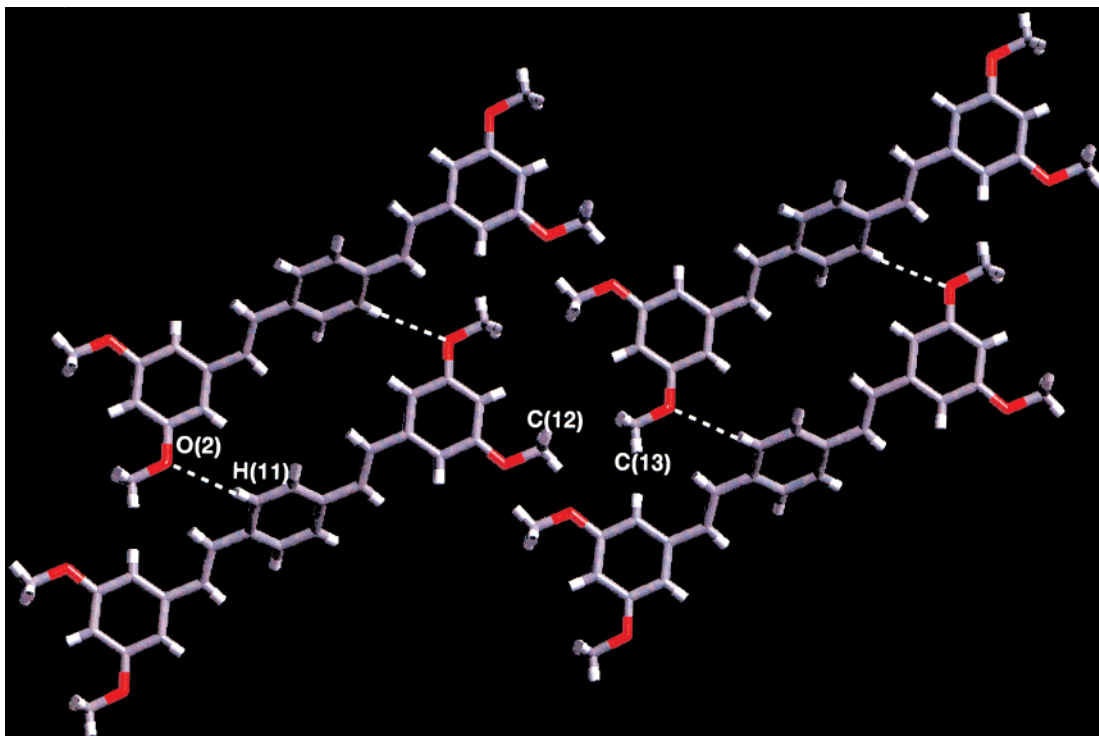


Figure 8. A layer of the structure of 1,4-bis(3,5-dimethoxystyryl)benzene (**5**) roughly in the *bc* plane. Annotated close contacts are of a distance of 2.69(4) Å.

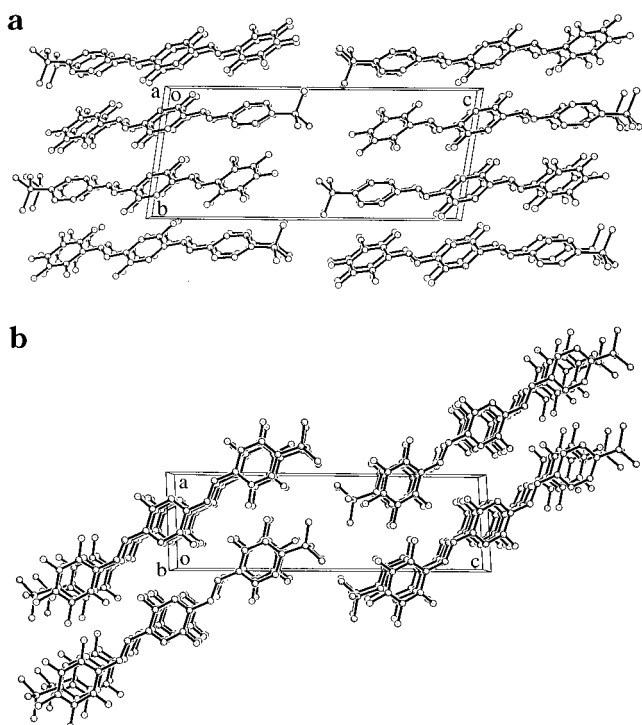


Figure 9. Packing diagram of 2,5-difluoro-1-(pentafluorostyryl)-4-(4-*tert*-butylstyryl)benzene (**6**) viewed down the (a) *a* axis and (b) *b* axis.

T_m for **5** is lower than **4**, consistent with **4** exhibiting four O \cdots H–C interactions per molecule in contrast to the two observed in the lattice of compound **5**. It is interesting to note the increase for **6** which contains phenyl-perfluorophenyl stacking and a network of weak F \cdots H–C interactions. Under atmospheric conditions, DMF is released from **7** leaving behind a dull orange solid. Although a full thermal analysis of **7** containing

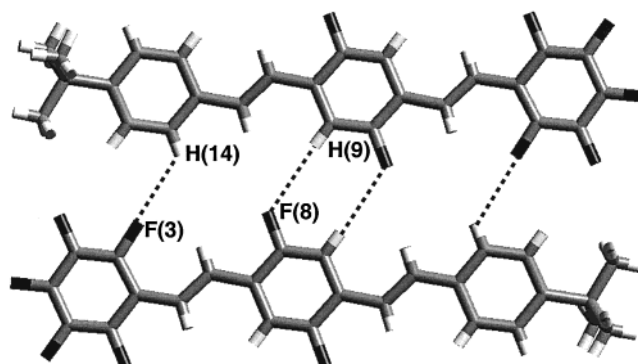


Figure 10. A layer of the structure of 2,5-difluoro-1-(pentafluorostyryl)-4-(4-*tert*-butylstyryl)benzene (**6**) roughly in the *bc* plane. Annotated close contacts are in shown in angstroms.

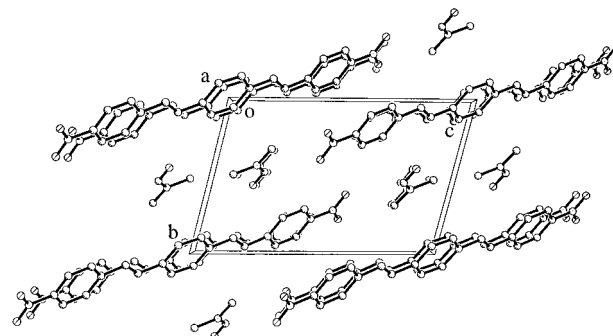


Figure 11. Packing diagram of 1,4-bis(4-nitrostyryl)benzene-2DMF (**7**) viewed down the *a* axis.

DMF in the lattice is beyond the scope of this work, the resulting material was also analyzed for rough comparison and is included in Table 3.

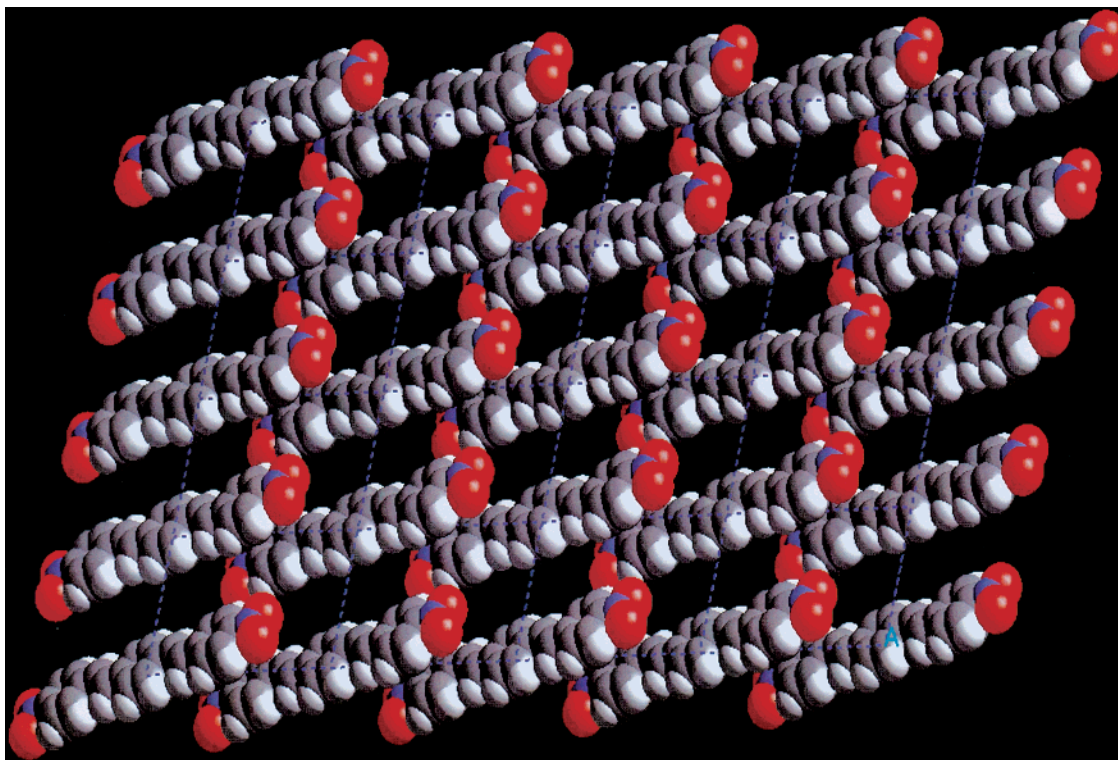


Figure 12. Packing diagram of 1,4-bis(4-nitrostyryl)benzene·2DMF (**7**) viewed down the *a* axis. DMF molecules have been removed to demonstrate the formation of channels within the lattice.

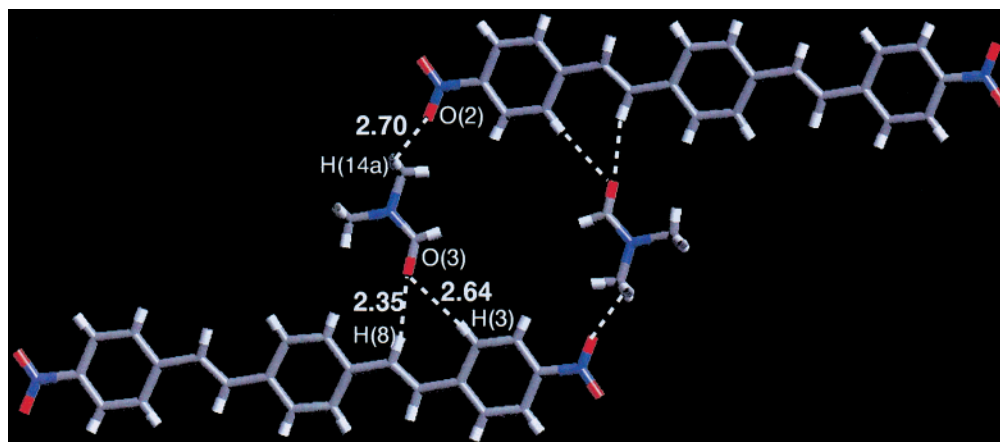


Figure 13. A layer of the structure of 1,4-bis(4-nitrostyryl)benzene·2DMF (**7**) roughly in the *bc* plane. Annotated close contacts are shown in angstroms.

Summary and Conclusions

As stated in the Introduction, a better understanding of chromophore–chromophore interactions in the solid state is an integral design component for novel anisotropic organic materials. The results reported herein highlight the diversity of arrangements available to a given conjugated framework with varying substitution patterns. For these DSB structures, a continuum between herringbone-like arrangements to coplanar stacks is demonstrated. The resulting lattices contain crystal engineering synthons that have been previously identified.²⁵ The lattices of **1** and **2** are characterized by aromatic ring interactions which result in edge-to-face

orientations between both intra- and intermolecular rings. Structures for **2** and **3** contain C–H···N interactions which have been recognized as hydrogen bonds.²⁶ These directional interactions lead to a more regular registry between chromophores and give rise to in a more symmetric lattice. The C–H···O interactions in **4** and **5** are due to electrostatic forces and also refine lateral registry between molecules. The end result is the formation of loose stacks within the lattice. In **6** phenyl/perfluorophenyl stacking and a lateral network of C–H···F interactions come together to form parallel cofacial stacks. Compound **7** contains polar NO₂ groups that have been used to form rigid frameworks for solvent inclusion.²⁴

(25) Desiraju, G. R. *Solid-State Supramolecular Chemistry: Crystal Engineering*. In *Comprehensive Supramolecular Chemistry*; Atwood, J. L., Davies, J. E. D., Macnicol, D. D., Vögtle, F., Eds.; Pergamon Press: Exeter, UK, 1996; Vol. 6, pp 1–22 and references therein.

(26) Reddy, D. S.; Goud, B. S.; Panneerselvam, Desiraju, G. R. *J. Chem. Soc., Chem. Commun.* **1993**, 663.

Table 1. Crystal Data and Refinement Parameters for 1,4-Bis(2,2-diphenylethenyl)benzene (1), 1,4-Bis(1-cyano-2,2-diphenylethenyl)benzene (2), 1,4-Bis(1-cyano-2-phenylethenyl)benzene (3) and 1,4-Bis(2,5-dimethoxystyryl)benzene (4)

crystal parameters	1	2	3	4
chemical formula	C ₃₄ H ₂₆	C ₃₆ H ₂₄ N ₂	C ₂₄ H ₁₆ N ₂	C ₂₆ H ₂₆ O ₄
formula weight	434.55	484.57	332.39	402.47
crystal system	triclinic	monoclinic	orthorhombic	monoclinic
space group (no.)	<i>P</i> $\bar{1}$ (no. 2)	<i>C</i> 2/ <i>c</i> (no. 15)	<i>Pbca</i> (no. 61)	<i>P</i> 2 ₁ / <i>n</i> (no. 14)
<i>Z</i>	2	4	4	2
<i>a</i> , Å	9.1077(9)	14.134(12)	6.815(3)	7.423(2)
<i>b</i> , Å	11.2130(11)	8.915(8)	7.191(3)	16.609(3)
<i>c</i> , Å	13.5850(13)	20.79(2)	35.198(14)	8.789(2)
α , deg	103.511(2)	90	90	90
β , deg	108.408(2)	98.08(2)	90	107.88(2)
γ , deg	103.496(2)	90	90	90
<i>V</i> , Å ³	1206.9(2)	2594(4)	1724.8(12)	1049.7
ρ_{calc} , mg/m ³	1.303	1.241	1.280	1.273
crystal dimens, mm	0.53 × 0.11 × 0.11	0.52 × 0.13 × 0.13	0.27 × 0.27 × 0.013	0.10 × 0.24 × 0.25
<i>T</i> , °C	-80	-80	-80	-80
2 θ range for data	2.0–50.0	2.0–50.0	2.0–50.0	2.0–50.0
total reflections	10889	5320	6478	6156
independent reflections	4237 [<i>R</i> ₁ (<i>F</i> ²) = 0.0244]	2269 [<i>R</i> ₁ (<i>F</i> ²) = 0.0984]	1132 [<i>R</i> ₁ (<i>F</i> ²) = 0.1123]	2425 [<i>R</i> ₁ (<i>F</i> ²) = 0.0244]
no. of observed data	4232 (<i>I</i> > 2 σ (<i>I</i>))	2269 (<i>I</i> > 2 σ (<i>I</i>))	2269 (<i>I</i> > 2 σ (<i>I</i>))	1941 (<i>I</i> > 2 σ (<i>I</i>))
no. of parameters varied	307	173	126	138
μ , mm ⁻¹	0.067	0.072	0.075	0.085
<i>R</i> ₁ (<i>F</i>), <i>wR</i> ₂ (<i>F</i> ²), (<i>I</i> > 2 σ (<i>I</i>))	0.0416, 0.0858	0.0585, 0.1297	0.0853, 0.2143	0.0402, 0.1012
<i>R</i> ₁ (<i>F</i>), <i>wR</i> ₂ (<i>F</i> ²), all data	0.0767, 0.0961	0.0816, 0.1348	0.1043, 0.2424	0.0525, 0.1073
goodness-of-fit on <i>F</i> ²	0.899	0.856	1.128	1.051

Table 2. Crystal Data and Refinement Parameters for 1,4-Bis(3,5-dimethoxystyryl)benzene(5), 2,5-Difluoro-1-(pentafluorostyryl)-4-(4-*tert*-butylstyryl)benzene (6) and 1,4-Bis(4-nitrostyryl)benzene·2DMF (7)

crystal parameters	5	6	7
chemical formula	C ₂₆ H ₂₆ O ₄	C ₂₆ H ₁₉ F ₇	C ₂₈ H ₃₀ N ₄ O ₆
formula weight	402.47	464.41	518.56
crystal system	triclinic	triclinic	triclinic
space group (no.)	<i>P</i> $\bar{1}$ (no. 2)	<i>P</i> $\bar{1}$ (no. 2)	<i>P</i> $\bar{1}$ (no. 2)
<i>Z</i>	1	2	1
<i>a</i> , Å	6.4762(5)	6.1188(3)	5.8989(5)
<i>b</i> , Å	8.4440(6)	8.5543(5)	8.8473(8)
<i>c</i> , Å	9.9979(7)	19.9386(10)	13.1992(11)
α , deg	80.1380(10)	98.631(2)	102.7830(10)
β , deg	76.8280(10)	91.026(2)	95.926(2)
γ , deg	76.1900(10)	99.201(2)	102.4260(10)
<i>V</i> , Å ³	513.00(6)	1017.59	647.76(10)
ρ_{calc} , Mg/m ³	1.303	1.303	1.329
crystal dimens, mm	0.52 × 0.46 × 0.40	0.50 × 0.10 × 0.13	0.53 × 0.12 × 0.12
<i>T</i> , °C	-80	-80	-80
2 θ range for data, °	2.0–50.0	2.0–50.0	2.0–50.0
total reflections	4570	4274	5791
independent reflections	1795 [<i>R</i> ₁ (<i>F</i> ²) = 0.0244]	2693 [<i>R</i> ₁ (<i>F</i> ²) = 0.0244]	2268 [<i>R</i> ₁ (<i>F</i> ²) = 0.0286]
no. of observed data	1795 (<i>I</i> > 2 σ (<i>I</i>))	2692 (<i>I</i> > 2 σ (<i>I</i>))	2267 (<i>I</i> > 2 σ (<i>I</i>))
no. of parameters varied	166	301	210
μ , mm ⁻¹	0.087	0.132	0.095
<i>R</i> ₁ (<i>F</i>), <i>wR</i> ₂ (<i>F</i> ²), (<i>I</i> > 2 σ (<i>I</i>))	0.0376, 0.1093	0.0748, 0.1581	0.0526, 0.1660
<i>R</i> ₁ (<i>F</i>), <i>wR</i> ₂ (<i>F</i> ²), all data	0.0398, 0.1120	0.1128, 0.1909	0.0650, 0.1781
goodness-of-fit on <i>F</i> ²	1.045	1.254	1.060

Table 3. Melting and Thermodynamic Data from DSC Analysis of Compounds 1–7

compound	<i>T</i> _m (°C ± 0.6)	ΔH_{fusion} (kJ mol ⁻¹ ± 0.8)
1	193.1	60.9
2	328.8	47.1
3	255.7	45.2
4	215.1	68.7
5	171.7	59.2
6	238.8	51.3
7 ^a	284.5	44.3

^a Sample did not include DMF as shown in crystal structure.

Although we are not at the stage of predicting the arrangement of the distyrylbenzene framework a priori, it is straightforward to rationalize the experimentally determined lattices in light of electrostatic interactions. Furthermore, different arrangements can be targeted

for specific applications. For example, the steric bulk and lack of cofacial aromatic fragments in **2** and **3** indicate potential applications as optoelectronic materials that avoid excimer formation. Layered cofacial stacks, as observed in **6**, have been shown to be the ideal morphology for organic field-effect transistors due to the expected higher charge mobility.²⁷ It is also noteworthy that the observed differences in the arrangement of the underlying DSB framework in these structures sets the 3-ring oligomer apart from its 5-ring counterpart. Known structures of 1,4-bis(4-styrylstyryl)benzene⁹ and derivatives²⁸ fall conveniently into two categories of packing: herringbone and coplanar.

(27) Laquindanum, J. G.; Katz, H. E.; Lovinger, A. J.; Dodabalapur, A. *Chem. Mater.* **1996**, *8*, 2542.

(28) Gill, R. E.; van Hutten, P. F.; Meetsma, A.; Hadziioannou, G. *Chem. Mater.* **1996**, *8*, 1341.

Experimental Section

General Details. All compounds were prepared using standard Schlenk techniques and were handled under yellow lights to avoid photooxidation and/or photopolymerization. All starting materials were obtained from Aldrich and were used as received. Compounds **1**, **4**, **5**, and **7** were prepared via Wittig condensation as described previously for distyrylbenzene derivatives.²⁹ Compound **2** and **3** was obtained by Knoevenagel condensation¹⁶ while compound **6** was prepared by Heck coupling.¹³

X-ray Structure Determination. Crystals were mounted onto thin glass fibers with epoxy resin and immediately placed in a cold nitrogen stream at 150 K on a Bruker SMART CCD diffractometer equipped with a normal focus, 2.4 kW sealed tube X-ray source (Mo K α radiation, $\lambda = 0.71073$ Å) operating at 45 kV and 40 mA. The temperature control was achieved with an Oxford Cryostream that could provide a temperature range from 80 to 375 K with a stability of about 0.1 K. The detector to crystal distance was set to 5.10 cm and the corresponding maximum 2θ angle was $\sim 56^\circ$. A full sphere of intensity data were collected in 2252 frames with ω scans (width of 0.30° and exposure time of 30 s per frame). The empirical absorption corrections based on the equivalent reflections were performed using the program SADABS and

other possible effects such as absorption by the glass fiber were simultaneously corrected.

The structures were solved by direct methods followed by successive difference Fourier methods. All calculations were performed using SHELXTL (version 5.0.3) running on a Silicon Graphics Indy 5000. Full-matrix refinements were against F^2 . Hydrogen atoms were calculated at idealized positions and their atomic positions were refined as riding atoms of their parent carbon atoms. The crystal data and refinement results are summarized in Tables 1 and 2. ORTEP drawings, positional coordinates, selected bond distances and further details of the data collection, solution and refinement can be found in the Supporting Information.

Differential Scanning Calorimetry. Differential scanning calorimetry was performed on a TA Instruments DSC 2920 Modulated differential scanning calorimeter. Samples were encapsulated in aluminum pans and were heated at a rate of 10°C per minute. Melting points were determined by extrapolation to baseline from the slope of the onset of the transition. Heats of fusion were determined by integration of the peak area for the melting transition.

Supporting Information Available: ORTEP drawings, positional coordinates, selected bond distances, and further details of the data collection, solution, and refinement. This material is available free of charge via the Internet at <http://pubs.acs.org>.

(29) Wadsworth, D. H.; Schupp, O. E.; Seus, E. J.; Ford, J. A., Jr. *J. Org. Chem.* **1964**, *30*, 680.

CM991194O